GND-254904, Fig. S1. Zhi, et al.

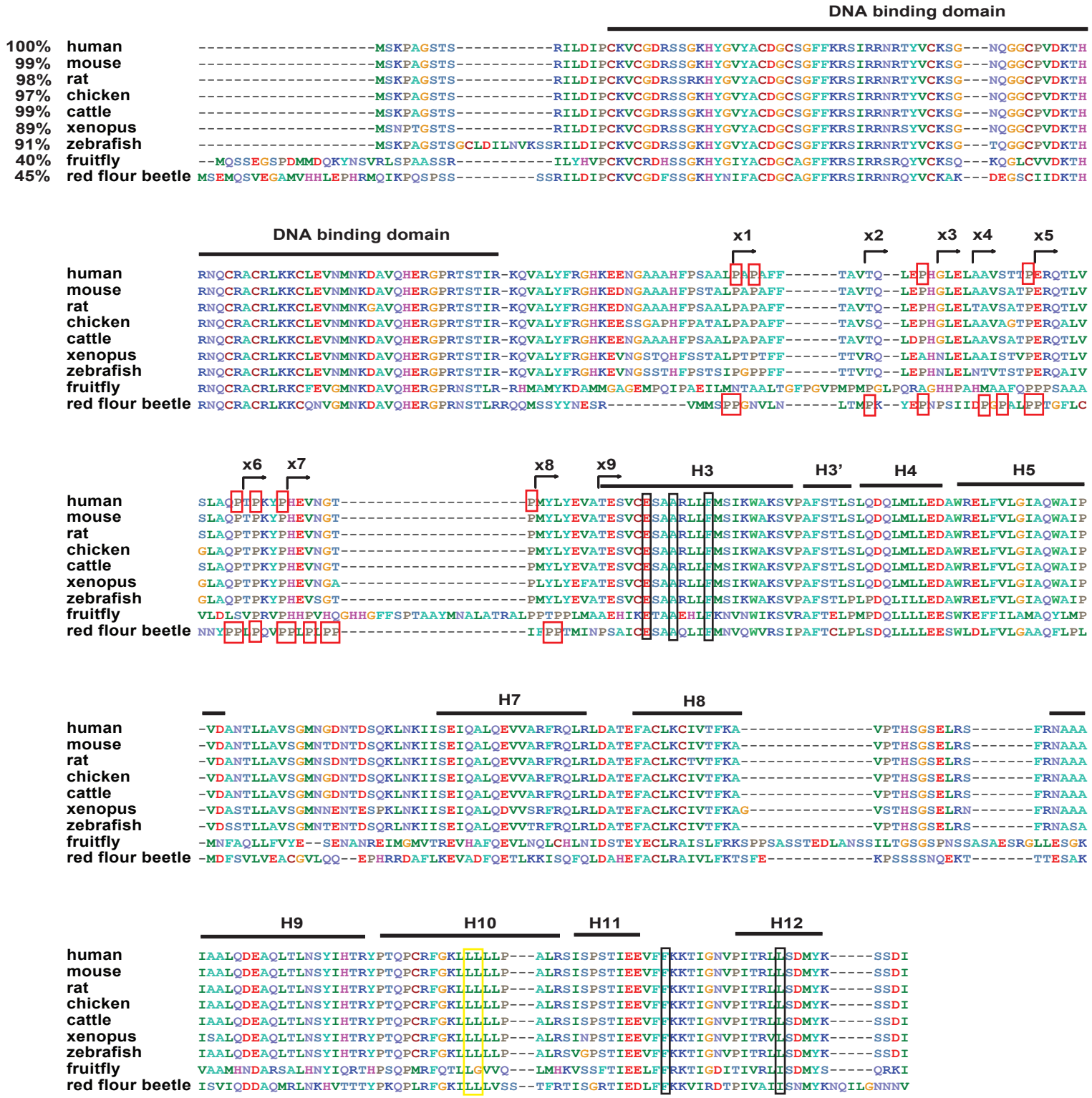

Supplementary Figure 1. The full length sequence alignment of TLX from human (NP_003260), mouse (NP_689415), rat (NP_001106668), chicken (NP_990501), cattle (NP_001179582), zebrafish (NP_001003608), xenopus (NP_001079280), fruitfly (NP_524596), and red flour beetle (NP_001034502). The percentages left to species stand for sequence identity to human TLX. TLX has the DNA binding domain, followed by the ligand binding domain that may not contain traditional helices H1 and H2. Helices H3-H12 are labeled by H and numbers. In front of helix H3, a series of human TLX N-terminal trunctions were made (designated by arrowheads and named the letter x followed by numbers). MBP-TLXx9 yielded initial crystals that were optimized by homologous surface mutations. Several prolines are present in front of human or red flour beetle TLX helix H3 and encircled by red boxes. They do not favor the formation of helices.The amino acids involved in TLX/Atrophin binding are conserved and encircled by black boxes. The residues potentially involved in TLX dimerization are encircled by yellow box.

GND-254904, Fig. S2. Zhi, et al.

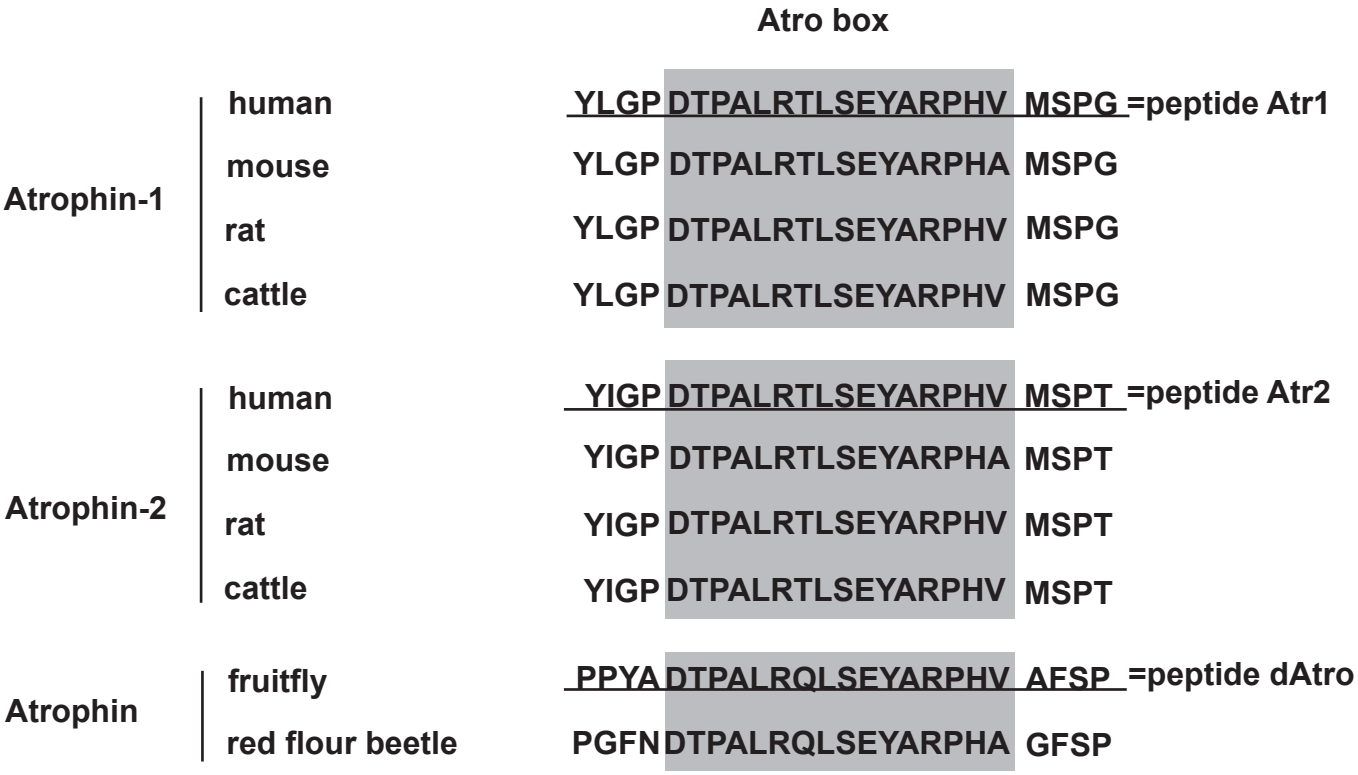

Supplementary Figure 2. The Atro box sequence alignment of Atrophin-1 from human (NP_001007027), mouse (NP_031907), rat (NP_058924), cattle (NP_001192677), Atrophin-2 from human (NP_001036146), mouse (NP_001078961), rat (NP_446337), cattle (XP_005217062), Atrophin from fruitfly (NP_659574) and red flour beetle (XP_008194914). The Atro box sequences are highlighted in grey. The peptide sequences used in crystallization and biochemical assays are underlined.

GND-254904, Fig. S3. Zhi, et al.

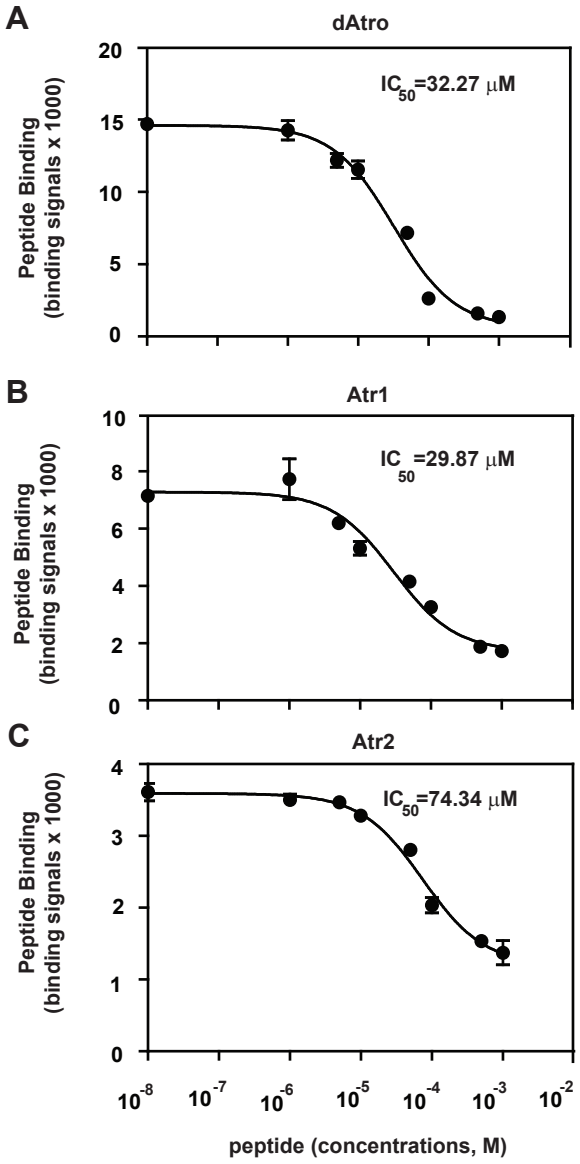

Supplementary Figure 3. Homologous competitive binding of peptides dAtro, Atr1 and Atr2 to TLXLBD in the AlphaScreen assay. Biotinylated dAtro (A), Atr1 (B) or Atr2 peptide (C) (200 nM) from Fig. 1a was incubated with the TLXLBD (residues 182–385) HisMBP fusion protein and increasing concentrations of nonbiotinylated dAtro (IC_{50} =32.27 μM), Atr1(IC_{50}=29.87 μM) or Atr2 (IC_{50}=74.34 μM) peptide . Error bars = SD (n = 3).

GND-254904, Fig. S4. Zhi, et al.

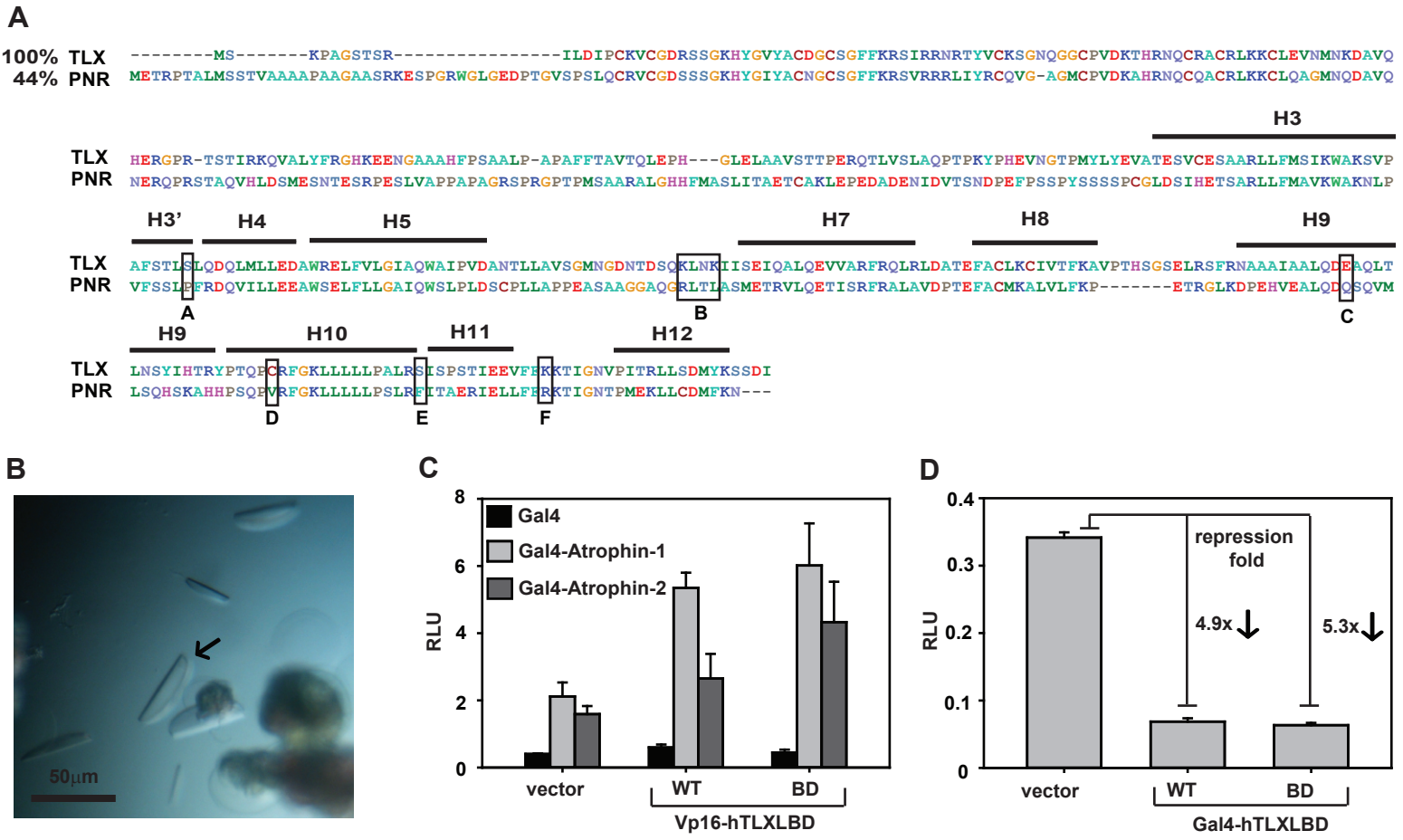

Supplementary Figure 4. Obtainment of diffractable human TLX (hTLX) LBD crystals using the homologous surface mutation strategy. (A) Based on Amino acid sequence alignment of human TLX (NP_003260) and PNR (NP_055064, PDB ID code 4LOG, sequence identity to TLX=44%, six sites (marked A–G) predicted to be on the TLX surface were mutated to the corresponding amino acids in PNR (circled in black box) individually or in combination. Helices H3-12 are labeled by H and numbers. (B) MBP-hTLXLBD-BD (the combinatorial mutations of sites B and D in TLX (residues 182-385) in complex with the peptide dAtro yielded half-moon-like crystals (pointed by arrowheads) that diffracted up to 3.55 Å). The crystals were grown at 20 °C in sitting drops containing 1.0 μL of the protein solution (10 mg/mL) and 1.0 μ L of the well solution containing 0.2 M sodium/potassium phosphate, 20% (wt/vol) PEG3350. (C) The combinatorial mutations of sites B and D did not affect the interaction between hTLX and Atrophin-1 or -2 in mammalian two hybrid assays. Mouse Atrophin-1 (residues 823-950) and mouse Atrophin-2 (residues1197-1334) were fused to Gal4. (D) The combinatorial mutations of sites B and D did not affect repressive activity of hTLX in cell reporter assays using the Gal4 fused receptor LBD. All error bars = SD (n = 3).

GND-254904, Fig. S5. Zhi, et al.

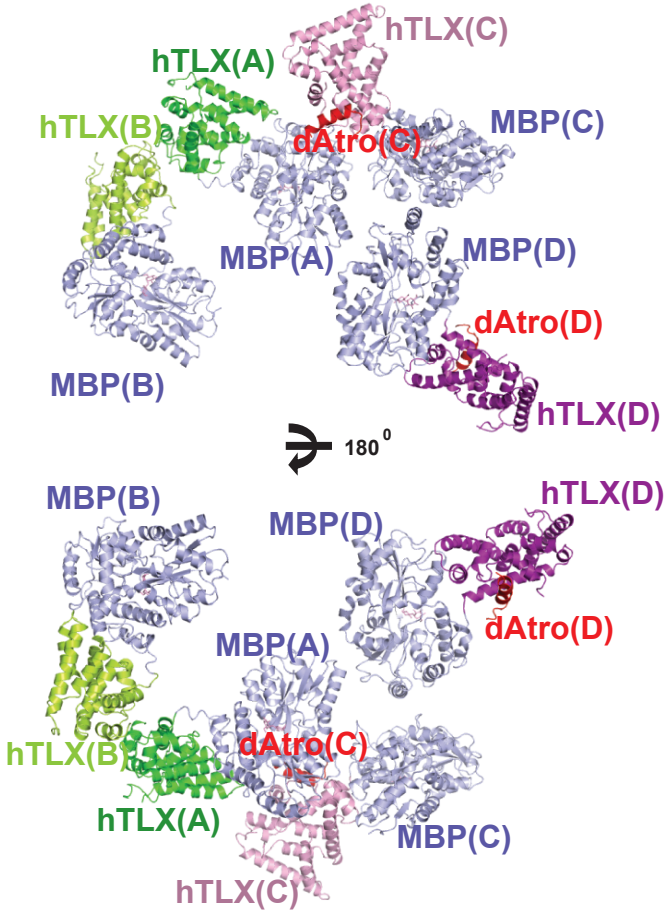

Supplementary Figure 5.There are four MBP (light blue) fused hTLX LBDs in one noncrystallographic symmetric unit. Two LBDs (TLX(C) in pink and TLX(D) in purple) are in complex with peptide dAtro (red) and arranged in a non-symmetric manner. The other two LBDs (TLX(A) in green and TLX(B) in light green) are not in complex with peptide dAtro and arranged in a symmetric manner.

GND-254904, Fig. S6. Zhi, et al.

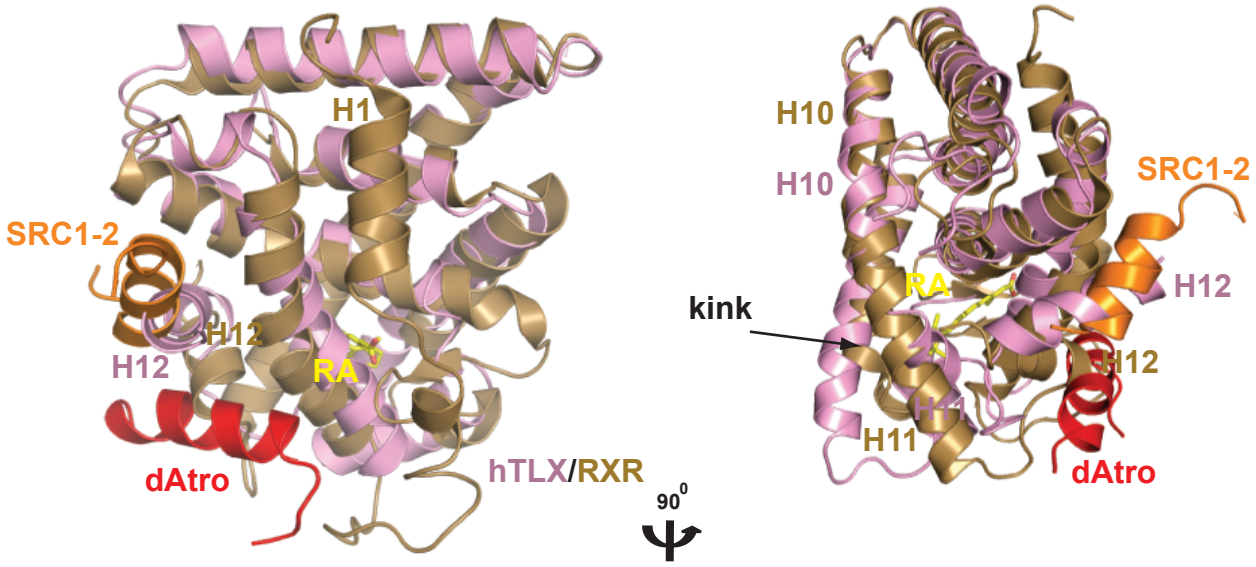

Supplementary Figure 6. Superposition of hTLX(pink) onto ligand-bound RXR (gold, PDB code=1FM6). Compared to RXR helices H10 and H11, there is a kink between TLX helices H10 and H11, which causes the space hindrance to ligand binding. RA , *cis*-retinoid acid in yellow, is ligand for RXR. hTLX does not have helix H1. Peptide dAtro clashes with RXR helix H12/H3.The RXR-interacting peptide SRC1-2 (orange) overlaps with hTLX helix H12.

GND-254904, Fig. S7. Zhi, et al.

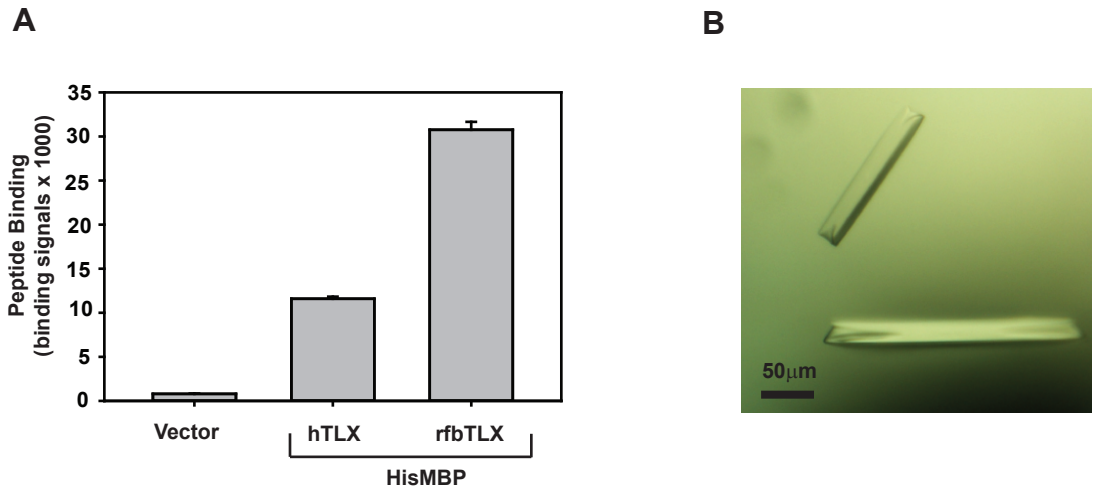

Supplementary Figure 7. Obtainment of diffractable insect TLX crystals. (A) red flour beetle TLX (rfbTLX) binds more strongerly than hTLX to peptide dAtro in an AlphaScreen assay. The TLX LBDs fused to HisMBP were used in experiments. Error bars = SD (n=3). (B) Representative picture of MBP-rfbTLX/dAtro crystals that diffracted up to 2.6 Å.The crystals were grown at 20 °C in sitting drops containing 1.0 μL of the protein solution (14 mg/mL) and 1.0 μL of the well solution containing 0.04 M citric acid, 0.06 M BIS-TRIS propane, pH 6.4, 20% (wt/vol) PEG3350.

GND-254904, Fig. S8. Zhi, et al.

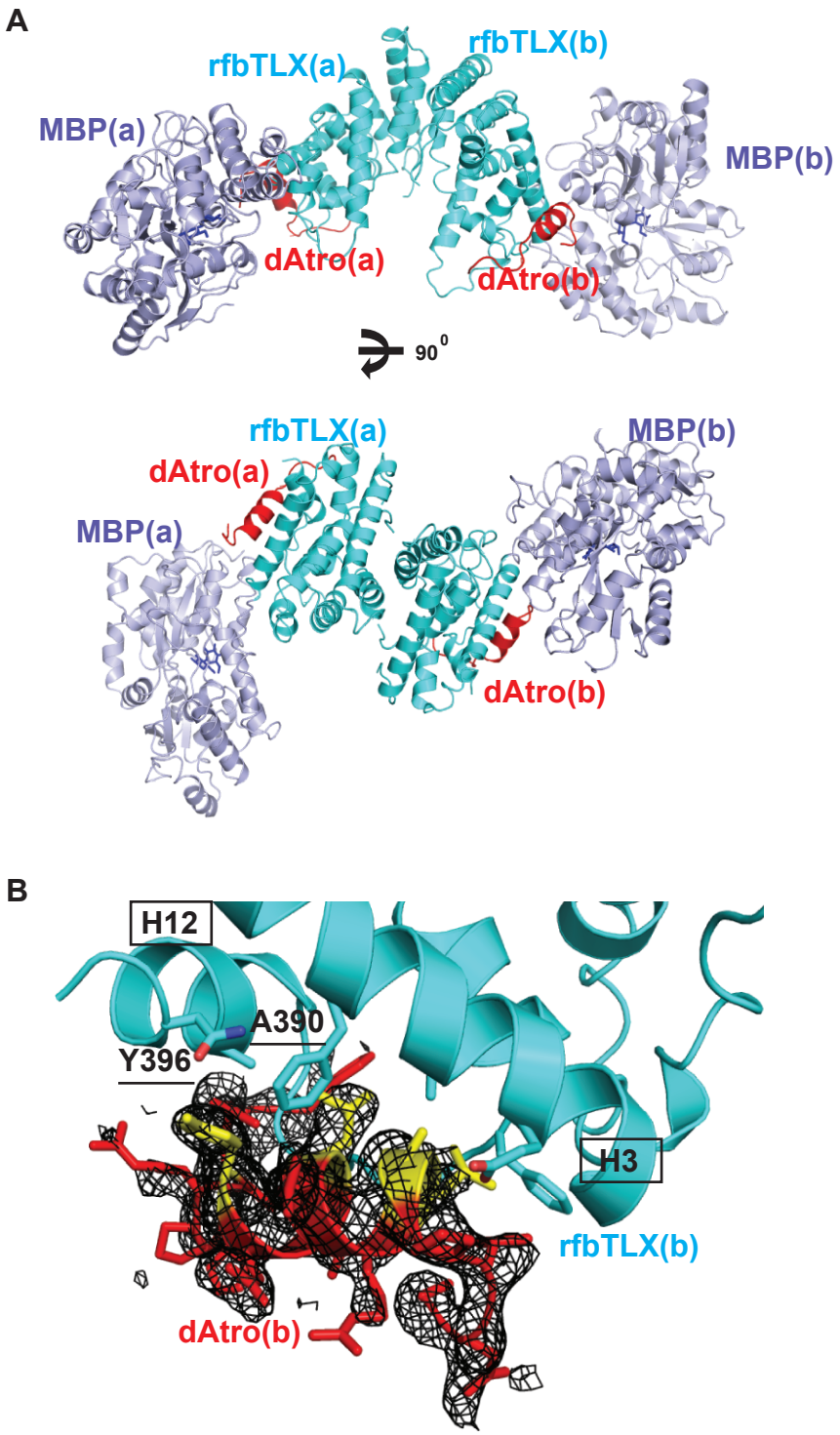

Supplementary Figure 8. Structural analysis of the red flour beetle TLX (rfbTLX) LBD. (A) There are two MBP (light blue) fused hTLX LBDs (cyan) in one noncrystallographic symmetric unit. Both are in complex with peptide dAtro (red) and form a symmetrical dimer via the helix H10-H10 interaction. (B) Representative Fo-Fc electron density omit map contoured at 1.0 σ for peptide dAtro(b) (red). Of note, the dAtrophin-contact residues on the rfbTLX(b) H12 are different from those on the rfbTLX(a) H12 and labeled.

GND-254904, Fig. S9. Zhi, et al.

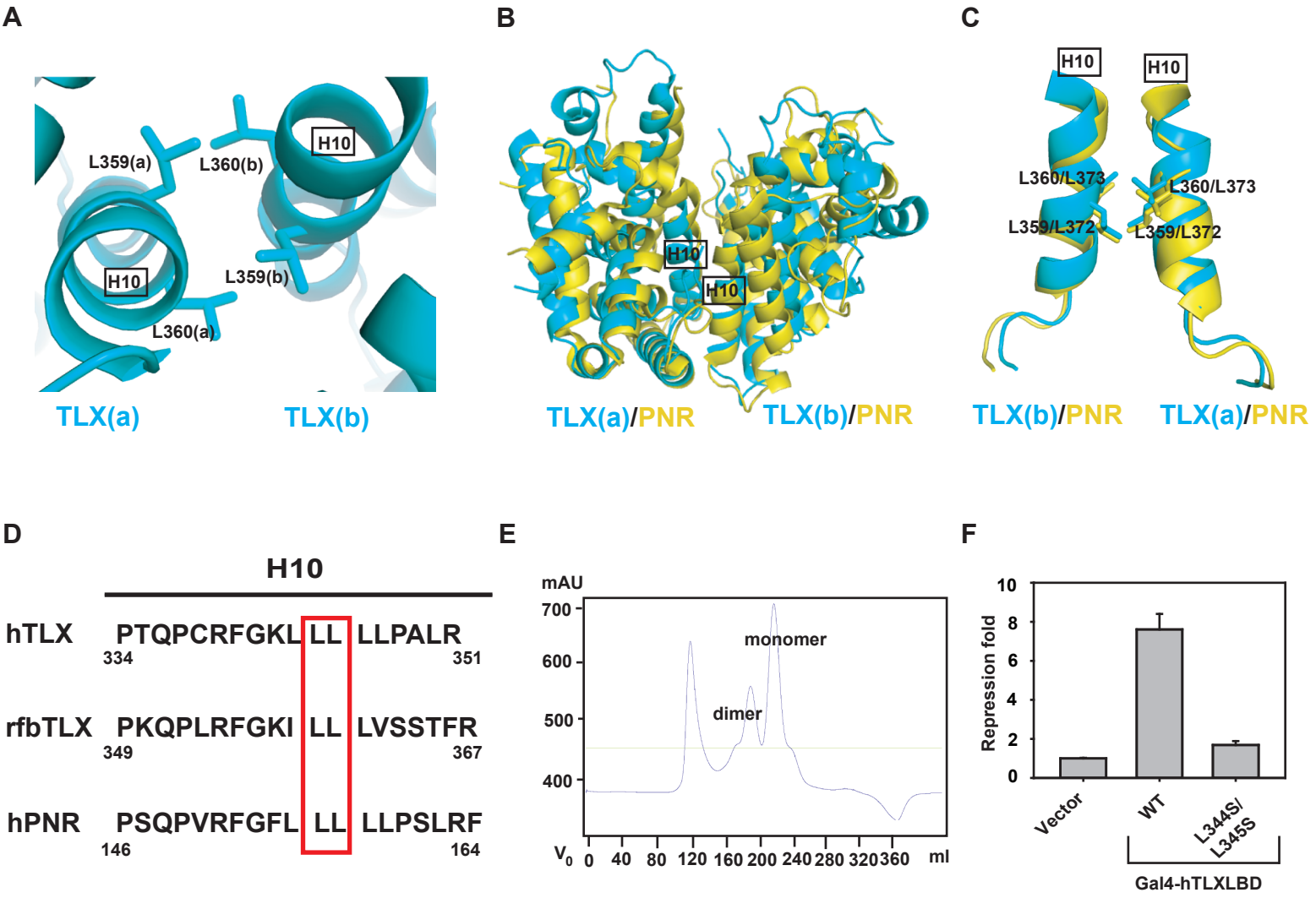

Supplementary Figure 9. Dimerization analysis of TLX. (A) The dimerization interface in rfbTLX is mediated by resiudes from helices H10 of both monomers. (B) Superposition of rfbTLX (cyan) and PNR (yellow). Dimerization in both receptors are mediated by the helix H10-H10 interaction. (C) Close-up presentation of the dimerization interface in superposed rfbTLX and PNR. The residues from helices H10 that form the dimer are conserved in rfbTLX and PNR. The first residue stands for rfbTLX and the second represents PNR. (D) The sequence alignment of helix H10 from hTLX, rfbTLX and hPNR. The residues involved in receptor dimerization are conserved and encircled by red box. *Numbers* refer to the amino acid position in receptors. (E) hTLX forms a dimer in a representative size exclusion chromatography profile. (F) Mutation of residues involved in hTLX dimerization impaired hTLX repressive activity.

GND-254904, Fig. 10. Zhi, et al.

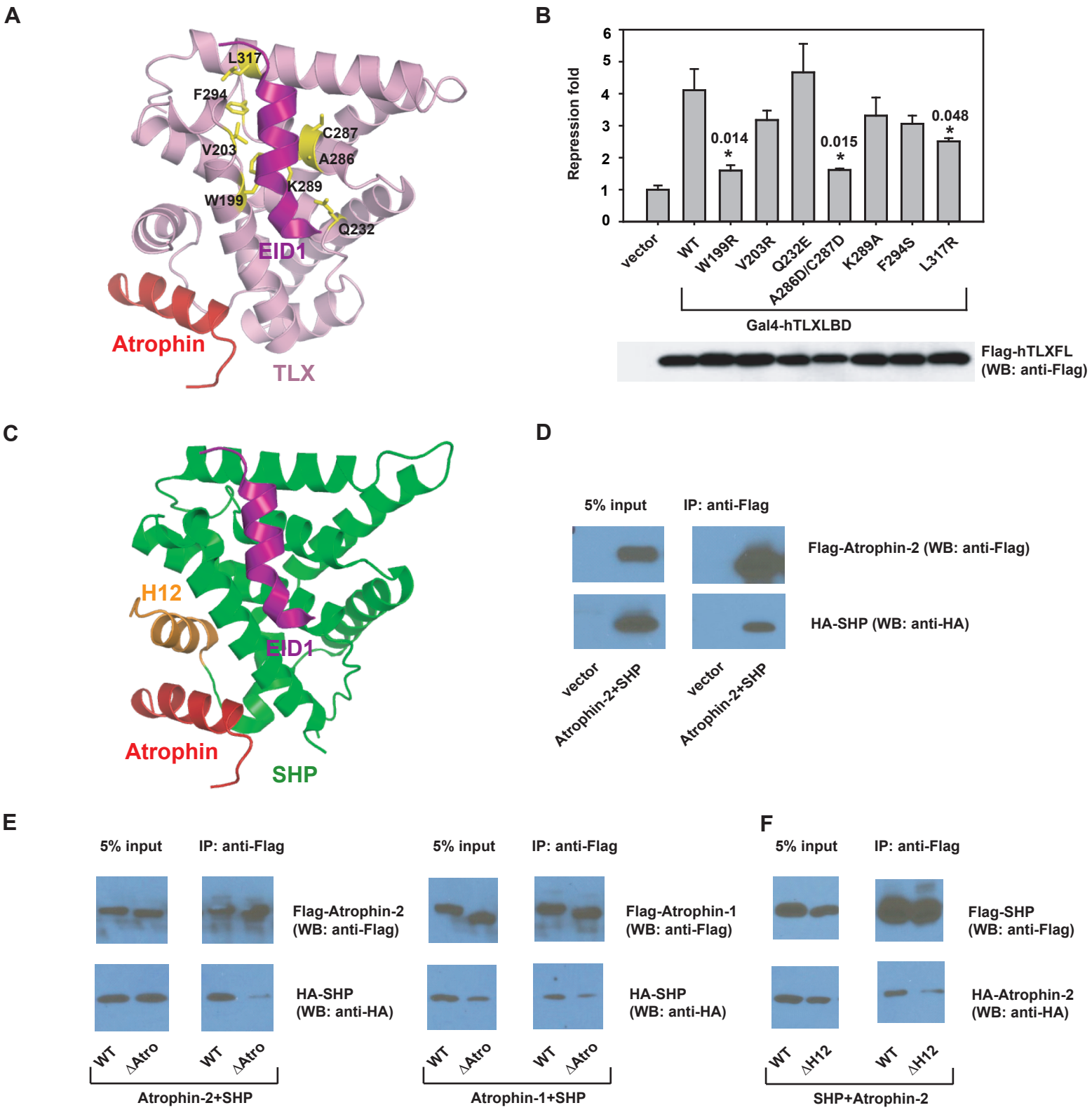

Supplementary Figure 10. Two unconventional modes of repression could be present in the same orphan nuclear receptor. (A) Superposition of hTLX (pink) and SHP (hidden)/EID1 (purple) reveals a potential H1 pocket in TLX. Residues that form this potential H1 pocket are highlighted in yellow and labeled. (B) Mutations in the corresponding TLX H1 pocket affected TLX repressive activity. Repression fold was calculated by comparing RLU with TLX to RLU without TLX. The results were then analyzed using Student's independent-sample t test. The statistical significance level was set to be $P < 0.05$ (one asterisk). The numbers above asterisks indicate P values. Error bars = SD (n = 3). Western blot was performed to check expression level of SHP mutants in cells. The same amount of cell lysates was loaded. (C) Superposition of SHP (green) and TLX (hidden)/Atrophin (red) reveals a potential auto-repressed pocket in SHP. (D) SHP (NP_ 035980) interacted with Atrophin-2 (NP_001036146, residues 1087-1566) in a co-immunoprecipitation assay. (E) Deletion of the Atro box (residues 1249-1264) in Atrophin-2 compromised the Atrophin-2-SHP interaction (left panel), while deletion of the Atro box (resiudes 879-894) in Atrophin-1 (NP_001007027, residues 720-1191) barely affected the Atrophin-1-SHP interaction (right panel). (F) Deletion of helix H12 in SHP decreased the Atrophin-2-SHP interaction.